

THERMAL BEHAVIOR OF HEXOGEN PHLEGMATIZED WITH MONTAN WAXES

M. Stanković¹, M. Blagojević² and S. Petrović²

¹Military Technical Institute of the Yugoslav Army, Katanićeva 15, 11000 Belgrade

²Faculty of Technology and Metallurgy, Karnegijeva 4, 11000 Belgrade, Yugoslavia

Abstract

Hexogen can be used pressed only if its crystals are covered by some polymeric material [1], either natural or artificial. Montan waxes, as natural polymeric materials, were used for the phlegmatization. The melting process of seven types of waxes was analyzed by differential scanning calorimetry. The thermal decomposition processes of hexogens and phlegmatized hexogens were investigated by dynamic differential scanning calorimetry and dynamic thermogravimetric analyses. Kinetic parameters of the decomposition processes of hexogens were evaluated by using data obtained from differential scanning calorimetric curves.

Keywords: differential scanning calorimetry, hexogen, kinetic parameters, montan wax, phlegmatization, thermogravimetric analysis

Introduction

Most explosive molecules, especially the important ones like hexogen (RDX, cyclo-trimethylene-trinitramine) or octogen (HMX, cyclo-tetramethylene-tetranitramine) cannot be used directly in powdered form as boosters or main charge explosives, principally because many of the powdered, even when compacted to high density, are too sensitive for military use [2]. A secondary reason, associated with those powders having acceptable sensitivity levels, is when compacted they do not always possess the physical characteristics permitting them to be pressed into stable, high quality charges which maintain their physical integrity over long periods of time.

Phlegmatization (or desensitization) of an explosive mean rendering it insensitive or less sensitive to the following actions: heat, shock, impact, percussion, or friction [3]. The explosive has to be desensitized to be comparable to that of either picric acid or trinitrotoluene (TNT) [4]. One of the ways to achieve desensitization of RDX is to coat the particles with wax [5], some artificial polymer (inert phlegmatizer) or a less sensitive explosive such as TNT [6, 7] (active phlegmatizer).

After production phlegmatized explosives are thermally characterized. Their melting temperatures, decomposition parameters and kinetics, as well as their thermal stabilities are determined by thermal analysis. The results of hexogen (RDX) examinations by dynamic differential scanning calorimetry (DSC) differ from each other and they are difficult to explain. The interpretation of the results is based on the influence of the combustion products, gases, on the condensed phase, as well as on

their acceleration and inhibition effects. Reliable data for the solid phase reaction are probably not available, due to autocatalytic and/or sublimation effects. These effects are explained by the hypothesis proposed for the nitrate esters, i.e., the 'cage effect' [1] induced inhibition due to radical-radical recombination. The proposed mechanism does not rule out the possibility of chain reactions, autocatalysis, or differences in the mechanism for different phases or in different temperature ranges. Activation energies of $E_a=133.95-142.32$ [8], $E_a=125.58-154.88$ [9] and $E_a=239.44$ kJ mol⁻¹ [10], a literature value of $E_a=198.84$ [11] and an experimental value of $E_a=282.14$ kJ mol⁻¹ [11] are known. The differences in E_a values, besides the above mentioned reasons, are probably due to the quality of various RDX, and especially the particle size distributions.

Experiments

Samples were analyzed using dynamic DSC and thermogravimetric analysis (TG). The experiments were performed on Perkin Elmer instruments, differential scanning calorimeter (DSC-4) and thermogravimetric analyzer (TGS-2), under a nitrogen flow of 50 ml min⁻¹. For the DSC analyses, samples of approximately 1 mg of explosives or 5 mg of waxes were hermetically sealed in Al pans. The temperature range was from 30 to 300 °C for the explosives and from 30 to 150 °C for the waxes, because the waxes do not have any peak, except the melting one, up to the RDX decomposition temperature. Before scanning, the wax samples were heated until completion of melting, then cooled down, and reheated. About 5 mg of explosive samples were taken for TG analyses. The heating rate (β) was always 10 °C min⁻¹, for both types of analyses.

Results and discussion

Four types of RDX were used, with various distributions of particle sizes. The highest content of the big particle sizes has RDX I, and the distribution of particle sizes is falling down from the biggest to the lowest for samples RDX I to RDX IV. RDX III consists of the particles which pass through the sieve of 315 and remain on the sieve of 140 μ m and RDX IV has particles lower than 140 μ m. Seven types of waxes were used for phlegmatization: HOECHST LP (LP), MWASK LP/2 (LP/2), HOECHST WE4 (WE4), HOEMST KSL (KSL), HOECHST KPS (KPS), HOECHST X22 (X22) and HOEFENST KFO (KFO). The characteristics of the phlegmatized explosives are given in Table 1.

The DSC curves of the melting processes of the waxes X22 and KFO are shown in Figs 1 and 2.

The values of the melting parameters of the waxes are given in Table 2.

The calculations of the rate constants, activation energies and reaction orders from the DSC curves are based on the Arrhenius equation:

$$k = Z e^{-E_a/RT}$$

where: k – the rate constant, 1 s^{-1} ; n – the order of the reaction; Z – the pre-exponential factor; R – the universal gas constant, $8.297\text{ J mol}^{-1}\text{ K}^{-1}$; T – temperature, K; and on the expression for the rate of a chemical reaction:

$$-dc/dt = kc^n$$

where c is the concentration of the reactant, mol dm^{-3} .

The value of c usually is obtained by the partial heat, $\Delta H_{\text{partial}}$, at time t , or temperature T . The values of ΔH and $\Delta H_{\text{partial}}$ are evaluated from the area under the DSC curve.

Table 1 Characteristics of phlegmatized explosives

Sample	Phlegmatized explosive	Type of wax	Type of RDX	Cont. of phlegm./mass%
1	RDX I/LP	LP	RDX I	4.87
2	RDX I/LP/2	LP/2	RDX I	4.50
3	RDX I/WE 4	WE4	RDX I	5.01
4	RDX I/KSL	KSL	RDX I	4.24
5	RDX I/KPS	KPS	RDX I	4.90
6	RDX I/X 22	X??	RDX I	4.89
7	RDX I/KFO	KFO	RDX I	4.91
8	RDX II/KFO	KFO	RDX II	4.62
9	RDX III/KFO	KFO	RDX III	4.76
10	RDX IV/KFO	KFO	RDX IV	5.01
11	RDX II/LP	LP	RDX II	4.94
12	RDX III/LP	LP	RDX III	4.88
13	RDX IV/LP	LP	RDX IV	4.73

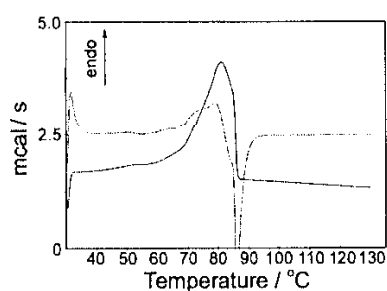


Fig. 1 DSC curve of montan wax X22; -- derivative

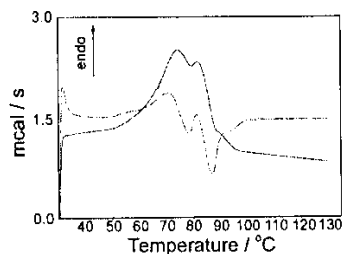


Fig. 2 DSC curve of montan wax KFO; --- derivative

Table 2 Melting parameters of the waxes

Sample	$T/^\circ\text{C}$				$\Delta H/J\text{ g}^{-1}$
	beginning	end	onset	max_{1-n}	
LP	46.99	86.76	67.65	81.85	181.05
LP/2	32.43	78.85	41.42	45.89/54.03	181.04
WE4	40.91	84.27	63.66	76.47	146.18
KSL	36.86	85.99	66.00	80.11	181.71
KPS	38.25	85.36	59.06	72.63/78.10	165.51
X22	54.17	87.54	68.99	81.80	156.35
KFO	39.50	97.84	59.53	74.86/81.50	155.34

$T_{\text{max}_{1-n}}$ — T of the melting peak maximum, or the maxima of a few peaks (multistep melting)

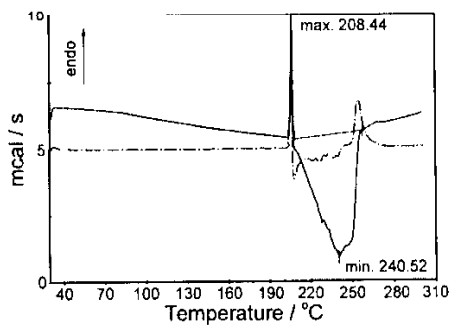


Fig. 3 DSC curve of phlegmatized hexogen, RDX-I/X22; --- derivative

Since there are three unknowns, k , E_a and n , to be determined, a multilinear regression must be performed.

The DSC and TG curves of the phlegmatized samples 6 (RDX-I phlegmatized with waxes X22) are given in Figs 3 and 4.

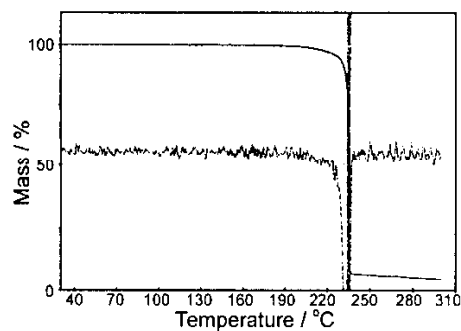


Fig. 4 TG curve of phlegmatized hexogen, RDX-I/X22

The decomposition and kinetic parameters of hexogen and phlegmatized hexogen (1–13) are given in Table 3.

The DSC curves of the first and second scans of the waxes have different shapes (number of peaks, T_{onset}). As the waxes were applied in the molten state for phlegma-

Table 3 Decomposition and kinetic parameters of the decomposition process of hexogen and the phlegmatized hexogen (1–13)

Sample	T_{onset} of the decomposition/ $^{\circ}\text{C}$	ΔH of the decomposition/ kJ kg^{-1}	$\ln k/ \text{s}^{-1}$	$E_a/ \text{kJ mol}^{-1}$	n
RDX I	206.5	-1726.7	42.4 ± 0.9	195.1 ± 4.2	0.9
RDX II	206.1	-2860.8	38.2 ± 0.8	177.1 ± 3.8	0.9
RDX III	206.1	-2466.3	39.0 ± 0.8	180.5 ± 3.9	0.9
RDX IV	206.9	-2063.2	42.1 ± 0.9	193.5 ± 4.2	0.9
1	206.9	-2484.2	27.6 ± 0.6	135.0 ± 2.9	0.5
2	206.9	-2182.6	31.8 ± 0.7	152.0 ± 3.3	0.6
3	206.9	-2393.6	32.4 ± 0.7	154.5 ± 3.3	0.5
4	206.9	-2388.4	28.8 ± 0.6	139.8 ± 3.0	0.5
5	207.3	-2442.4	28.4 ± 0.6	138.3 ± 3.0	0.4
6	207.7	-2528.6	27.3 ± 0.6	133.4 ± 2.9	0.5
7	206.9	-2676.1	25.3 ± 0.5	125.5 ± 2.7	0.5
8	206.5	-2618.1	33.9 ± 0.7	160.6 ± 3.5	0.6
9	206.9	-2531.7	31.7 ± 0.7	151.6 ± 3.3	0.6
10	206.5	-2427.4	31.4 ± 0.7	150.3 ± 3.2	0.6
11	206.5	-2663.8	28.0 ± 0.6	136.6 ± 2.9	0.5
12	206.8	-2368.8	28.6 ± 0.6	139.1 ± 3.0	0.4
13	206.1	-2356.6	29.4 ± 0.6	142.1 ± 3.1	0.4

tization of RDX, the scans of the second heating were recorded. Every melting peak of the waxes is asymmetric and broad. The temperatures of the beginning of melting range from 32.4 to 54.2°C, with the process being completed between 78.8 and 97.8°C. The melting intervals range from 33.3 (X22) to 58.3°C (KFO). Waxes with a broad melting range are easier to apply on the crystal surface than those with a narrow melting range. The former usually possess excellent coating properties. Samples LP/2, KPS and KFO exhibit multiple melting, the peak maxima are close to each other ($\Delta T_{\max LP/2}=8.1^\circ\text{C}$, $\Delta T_{\max KPS}=5.5^\circ\text{C}$, and $\Delta T_{\max KFO}=6.6^\circ\text{C}$). The DSC curves show only melting peaks up to 204°C. The waxes are stable up to the melting temperatures of RDX, which is important for their applications. However, what is obvious from these analyses, is the fact that some of the waxes have an extremely low melting temperature. In addition to the good properties of waxes, like their compatibility with explosives, broad melting ranges and good processability, they also have to fulfill the military specifications regarding exudation.

The DSC curves of RDX are characterized by two peaks, the first, endothermic peak of melting, overlaps with the second, exothermic peak of decomposition. The melting peaks are symmetric, with almost the same onset temperature value $\approx 204^\circ\text{C}$, ($203.3 \leq T_{\text{mel}} \leq 204.1$). The decomposition peak starts about 206°C. The values of ΔH decrease with diminishing grain size. The ΔH decomposition values of sample RDX I and RDX II are remarkably higher and lower compared then to the ΔH values RDX III and RDX IV probably because of the various particle size distributions. RDX III and RDX IV are composed of the particles from 315–140 μm and lower of 140 μm respectively. With phlegmatization the way of decomposition process is changed because of the wax presence. There are not significant differences between the T_{onset} values for the melting and decomposition processes of phlegmatized and unphlegmatized RDX. Differences exist, however, between the kinetic parameters, with the values of $\ln k$ and E_a increasing with decreasing grain sizes of RDX, but the reverse is with n . The $\ln k$, E_a , and n values for the phlegmatized samples are lower than for unphlegmatized RDX. It seems as though the decomposition reaction was slower for phlegmatized RDX than for unphlegmatized, probably because of the molten wax layer on the surface of the undecomposed grains of RDX, which slightly inhibits the reaction. Regarding the influences of the various grain sizes of RDX phlegmatized with the same wax, there is no regularity (samples 7–10, and 1, 11–13) in the dependence of the kinetic parameters on grain sizes.

The results of the TG analyses of hexogen (RDX) and phlegmatized hexogen (1–13) are shown in Table 4. Thermogravimetric examinations of RDX and the phlegmatized RDX samples showed that there was no mass loss from 30 to 180–190°C, and the samples lost a few mass% up to 206°C (i.e. the decomposition temperature of RDX from DSC measurements), and after $T_{\text{decomposition}}$ there is a sudden mass loss. After this rapid mass loss, there is an inflection point on the TG curve. More than 90 mass% of the explosive mass is transformed into volatile matter. The value of $T_{\text{inflection}}$ is lower for phlegmatized compared to unphlegmatized RDX. The mass lost is 2–3 mass% from $T_{\text{inflection}}$ to final temperature of examination. The solid residue is between 0 and 2.85 for RDX, increasing to 5.68 mass% for phlegmatized RDX. The existence of a solid residue of about 5 mass% is caused by the presence

Table 4 Results of the TG analyses of hexogen (RDX) and the phlegmatized hexogen (1–13)

Sample	$T_{\text{inflection}}/$ $^{\circ}\text{C}$	Δm from 206.6 $^{\circ}\text{C}$ to $T_{\text{inflection}}/$	Solid residue after $T_{\text{inflection}}/$	Solid residue on 300 $^{\circ}\text{C}/$
			mass%	
RDX I	243.7	90.3	5.6	2.8
RDX II	246.6	95.7	1.2	0.0
RDX III	246.6	93.8	4.7	1.7
RDX IV	250.0	95.8	3.0	1.0
1	237.8	95.8	7.0	1.0
2	234.4	91.8	3.4	5.0
3	234.7	93.1	3.9	1.0
4	235.2	90.9	7.5	4.7
5	236.9	92.0	6.0	3.7
6	236.1	92.1	6.8	4.6
7	235.7	92.3	6.5	3.6
8	233.6	90.0	7.5	5.4
9	238.2	92.0	6.4	3.2
10	237.8	91.7	6.9	4.8
11	239.5	91.4	6.8	4.6
12	238.7	93.6	4.9	2.3
13	239.5	91.2	8.0	5.8

of the waxes (with their 'minus' oxygen balance) and is connected with the wax distribution in the sample of 5 mg. For some samples, the solid residue was almost equal to the wax content in the phlegmatized RDX.

RDX loses mass more slowly with diminishing grain size. Phlegmatized RDX starts losing mass at lower temperatures. The grain size distribution has no influence on this process.

Conclusions

The width of the melting peak of the wax is important for the process of phlegmatization. From this point of view, KFO is the best with the broadest melting peak, and X22 the worst compared to the others. A very low T_{onset} of melting is not a desirable property of a wax. The wax LP/2 has the lowest T_{onset} . These two characteristics can be seen from the DSC curves. Other quality demands, like compatibility, exudation, etc., prescribed in military specifications, will determine the choice of the wax.

The grain size distribution of RDX has an influence on the kinetics of decomposition and on the mass lost during dynamic examination by DSC and TG. The $\ln k$ value increases from 38 to 42 l s^{-1} , and E_a increase from 177 to 193 kJ mol^{-1} with increasing content of smaller particles. The order of the reaction decreases slightly from 0.91 to 0.87. The decomposition reaction is slower after phlegmatization and the kinetic parameters have lower values. For the smaller granulations of RDX (i.e. RDX IV), the exothermic effects of the decomposition process of the phlegmatized RDX become greater.

The mass loss process during programmed heating of the samples depends on the grain size distribution of the RDX. With increasing content of smaller particles, RDX starts to lose the mass at higher temperatures. Phlegmatized RDX starts to lose mass at lower temperatures, compared to unphlegmatized samples. This means that RDX phlegmatized with waxes has a slightly lower thermal stability compared to RDX. The solid residues, at the final temperature of examination, varied from 0 to 2.85 mass% for RDX, increasing to 5.84 mass% for phlegmatized RDX, which is almost the same value as the wax content in phlegmatized RDX (the higher solid residues for phlegmatized RDX compared to RDX were expected because the waxes have a 'minus' oxygen balance. For explosive materials and their ingredients a 'minus' oxygen balance means the presence of the elementary carbon, hydrogen, carbon(II)-oxide, hydrocyanic acid, and etc. in decomposition products. There is not enough oxygen to transform the elementary carbon and hydrogen in carbon(IV)-oxide and water in decomposition products.) The various grain size distributions of RDX, taken for phlegmatization, have no influence on the beginning of mass loss.

References

- 1 H. Schmid, *J. Hazardous Materials*, 13 (1986) 89.
- 2 E. Anderson, 'Tactical Missile Warhead', 155 (1993) 81.
- 3 N. Lindstrom, US pat., 5,067,996 (1991).
- 4 Selim-H. Min. and J. K. Iskandar, 'Cold Regions Research and Engineering Lab', Hanover, NH, (1994).
- 5 P. W. Linder, 'Physics and Chemistry of Solid', Cavendish Laboratory, Cambridge (1996).
- 6 P. Waniger, *ICT*, 21 (1990) 1.
- 7 M. Kobayashi, *Jan.*, Kokai Tokyo Kōso J.P.02,271,986 (1990)
- 8 K. Kuo and M. Summerfield, *Fundamentals of Solid Propellants Combustion*, American Institute of Aeronautics and Astronautics, 90 (1984) 205.
- 9 S. Palopi and T. Brill, *Combustion and Flame*, 72 (1988) 153.
- 10 J. Dahn, *J. Hazardous Materials*, 4 (1980) 121.
- 11 R. N. Rogers and E. D. Morris, *Anal. Chem.*, 38 (1966) 412.